An Active Electrode Design for Weak Biosignal Measurements

Ning Ji[a b], Yanbing Jiang[a], Zijian Yang[a], Xiaobei Jing[a], Hui Wang[a], Yue Zheng[a], Zeyang Xia[a], Shixiong Chen[a]*, Lisheng Xu[b] and Guanglin Li[a]*

a Key Laboratory of Human-Machine Intelligence-Synergy Systems, Shenzhen Institutes of Advanced Technology, Chinese Academy of Sciences, Shenzhen, Guangdong 518055, China

b Sino-Dutch Biomedical and Information Engineering School, Northeastern University, Shenyang, Liaoning 110819, China

gl.li@siat.ac.cn, sx.chen@siat.ac.cn

***Abstract*—High quality and ambulatory measurements of biosignal, especially some weak biopotential signals with amplitude less than 1 μV is significant for the follow-up applications and is still challenging. This paper presents a new low-noise, high-performance active electrode design for such weak biosignal measurements. The proposed active electrode is designed in the fully-differential configuration in combination with the right-leg driven signal, which is seldom included in the previous design of active electrodes. Main advantages of this design lie in further improving the common-mode interference rejection with introducing right-leg driven signal and ideally driving differential inputs of ADS1299 to extract 1 μV level biosignal from other large noises voltages with the fully-differential configuration. The active electrode achieves 4.52 μVrms (0.5 – 200 Hz) input referred noise and 96.09 dB CMRR at 10Hz. Two preliminary verification experiments of ECG and EMG were performed using the traditional passive electrodes and the proposed active electrodes for comparison. The results demonstrated the benefits of the active electrode in terms of main interference suppression like power line interference and motion artifacts over the passive electrode. Therefore, the proposed active electrode with low noise and high CMRR could be used in weak biosignal (1 μV level) measurements in the future.**

Keywords—Active electrode; fully-differential; right-leg driven; instrumentation amplifier; weak biosignal measurement.

I. INTRODUCTION

There has been a growing demand for ambulatory biosignal (ECG, EEG, EMG, etc.) monitoring and measurements for human's daily healthcare [1], accurate diagnosis of diseases, rehabilitation and other personalized applications like brain-computer interfaces. Hence, high quality measurements of biosignal, especially some weak biopotential signals with amplitude less than 1 μV is essential and challenging for the follow-up medical evaluation and applications. Auditory brainstem response (ABR) is the one of such weak biosignal with its amplitude less than 1 μV or even 0.5 μV mostly. It is the voltage change recorded on the surface of the brain in response to acoustic stimuli, which is one of the weakest EEG signals. In reality, measurements of ABR is the most frequent way for the early detection of hearing loss. However, there are limitations existed in nowadays ABR measurements, for instance, it is time consuming and should be restricted in the standard electromagnetic shielding room, otherwise the ABR signal obtained is unstable and unreliable.

One of the reasons that cause the above limitations is the use of passive electrodes. Though, they have been widely used in the clinic for years as its mechanical simplicity, problems were found in biosignal measurements. The significant length of connection cable between the electrode (high impedance biosignal source) and the measurement circuit module could easily introduce 50/60Hz power line interference to the obtained signal [2]. In case of this, using active electrodes, which were defined as the electrodes that utilize impedance transformation at the sensing site through active electronic devices or circuits [3], is a superior solution for the problems that the cables brought [4]. With the minimal signal path length between the electrode and the first amplifier stage [1, 4], the input impedance of an active electrode could remain highest possible while the low output impedance (less than 1 Ω, compared with tens or even hundreds of kΩ of a passive electrode) could well match the low input impedance of the Analog-to-Digital converter (ADC), ensure that the signal measured is fully insensitive to the main interferences like cable motion artifacts, power-line interference [1] and get rid off the expensive, delicate shielded cables [4]. Nevertheless, it's not enough for weak biosignal measurements since the voltage buffers co-integrated with the active electrodes only act as impedance converters [1] which do not amplify the weak biosignal like ABR. Thus it is more recommended to perform signal amplification and other analog signal processing as close to the electrode as possible or even at the electrode [2]. Besides, to keep the input referred noise of electrode at an acceptable level, a power consuming instrumentation amplifier or a high-resolution ADC is still needed [1]. Therefore, the circuit of active electrode should be delicately designed for weak biosignal measurements. Previous literatures on active electrodes have focused mainly on ECG and EMG recording, which have demonstrated its better performance than passive electrodes with high-quality recording [5-8]. However, few reports of ABR studies with active electrodes were found.

This paper proposes a high-performance, low-noise active electrode design for weak biosignal measurements aiming at restraining common-mode interference such as power-line interference and other electromagnetic interference, as well as overcoming the effects of baseline drift and motion artifact

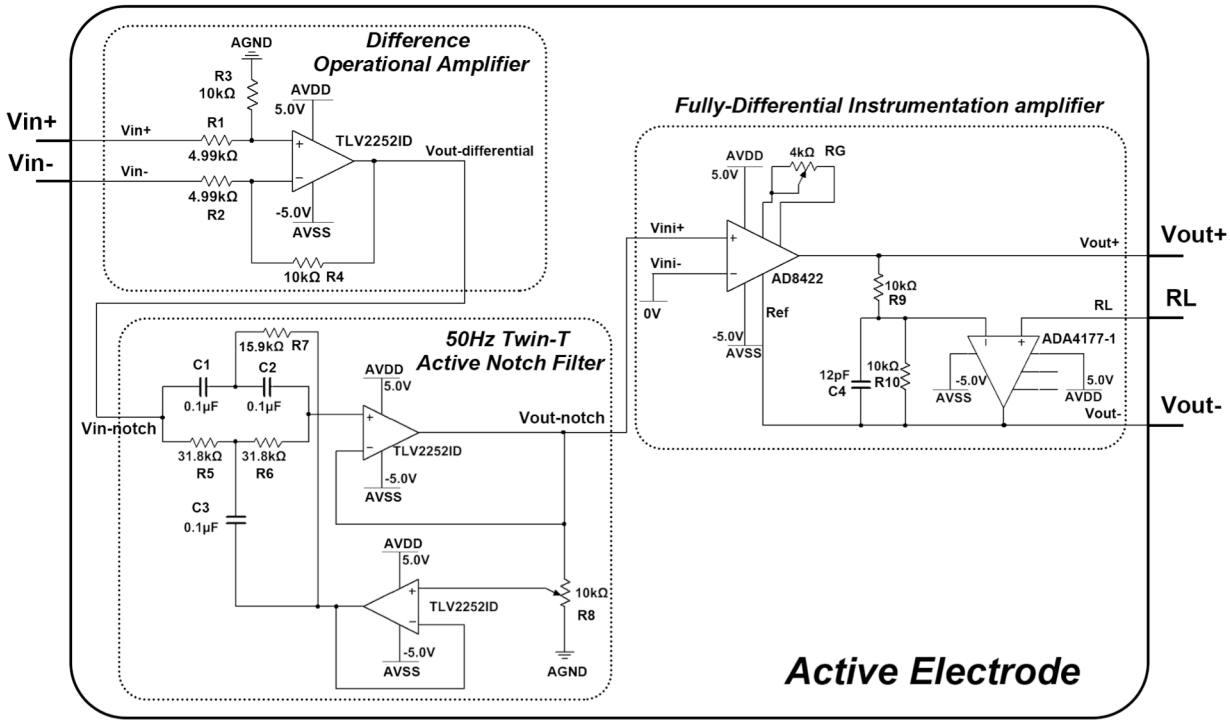

Fig. 1. The full circuit schematic of the proposed active electrode.

during measurements. Thus, the signal-to-noise ratio (SNR) of the detected biosignal could be improved. Specially, in combination with the right-leg driven signal, the proposed active electrode was designed in the fully-differential configuration which could seamlessly cooperate with ADS1299 to extract 1 μV level biosignal from other large noises voltages and further improve the common-mode rejection ratio (CMRR). Thus, the proposed active electrode could be applied in weak biosignal measurements like ABR monitoring applications.

II. Circuit Design and Description

A. Proposed Active Electrode Architecture

The proposed active electrode mainly consists of three circuit modules, which are the difference operational amplifier at the first stage, secondly the 50 Hz twin-T active notch filter with adjustable notch depth and finally the fully-differential instrumentation amplifier in combination with the right-leg driven signal. The full circuit schematic of the proposed active electrode is shown in Fig. 1.

The difference operational amplifier at the first stage is responsible for impedance matching and common-mode interference removing by developing an amplified single-ended differential output voltage from the two pole input signals (see Section Ⅱ-B).

The 50 Hz twin-T active notch filter with adjustable notch depth at the second stage is responsible for removing power line interference from the capacitive coupling of electrode wires, human body and the environment around the electromagnetic field, as the power line interference with large voltages (mV level or more) is the main interference during weak biosignal recording (see Section Ⅱ-C).

The fully-differential instrumentation amplifier, as the final and the most important stage of the proposed active electrode, mainly aims to provide increased immunity to the external common mode interference and twice the output swing for a given voltage limit when compared to the single-ended output [9]. Besides, by introducing the right-leg driven signal into the reference terminal of the instrumentation amplifier, the common mode output voltages could be precisely set and not easily affected by other interference except for the reference voltages. Moreover, it's well suited for driving differential ADC inputs and providing easy means for antialias filtering [9] which could seamlessly connect ADS1299 (see Section Ⅱ-D).

B. Difference Operational Amplifier

The difference operational amplifier stage is designed based on a standard subtractor circuit, which converts the two pole inputs to a single-ended differential output signal and then amplifies it. As shown in Fig. 1, the transfer function of the difference operational amplifier is

$$V_{\text{out-differential}} = -V_{\text{in}-}\left(\frac{R4}{R2}\right) + V_{\text{in}+}\left(\frac{R3}{R1+R3}\right)\left(\frac{R2+R4}{R2}\right) \quad (1)$$

Since R1=R2, R3=R4, the differential output could be simplified into

$$V_{\text{out-differential}} = \frac{R4}{R2}(V_{\text{in}+} - V_{\text{in}-}) \quad (2)$$

where the signal gain ratio is 2.004. Thus the two pole inputs V_{in+}, V_{in-} measured by two recording electrodes are converted into the single-ended differential output with 2.004 gain ratio. And the high input impedance is transformed into low output impedance which is not easily susceptible to the cable motion artifacts or power-line interference. As this main interference generated from the capacitive coupling among the conductors usually appears as common-mode signal, and the CMRR is directly proportional to the resistor matching error [9], thus choosing precision and symmetrical resistors is important to have good CMRR performance. A rail-to-rail, very low-power (34 μA) operational amplifier TLV2252 (Texus Instruments, Inc.) is used in our circuit. Exhibiting high input impedance and low noise ($19\text{nV}/\sqrt{\text{Hz}}$) with rail-to-rail output performance for increased dynamic range, TLV2252 is excellent for low level signal measurements from high-impedance sources.

C. 50 Hz Twin-T Active Notch Filter

Although the common-mode noises like 50 Hz power-line interference could be rejected with the differential structures, they still exist and may transform to differential-mode signals with the limitation of CMRR in reality, which could heavily affect the quality of the measured biosignal. Thus active notch filter for removing 50Hz power-line interference is necessary. This stage is designed based on the twin-T active notch filter circuit, as shown in Fig. 1. The center frequency of the notch filter was set as

$$f_r = \frac{1}{2\pi \times 31.8\text{k} \times 0.1\mu} = 50.07\text{Hz} \quad (3)$$

The quality factor Q is adjustable by switching different values of the resistor R8 (10kΩ maximum), and the notch depth of the center frequency is also adjustable, which is demonstrated as follows

$$Q = \frac{f_r}{BW} \quad (4)$$

where BW is the bandwidth of the stop band. Thus, the notch depth is in inverse proportion to the quality factor Q as it is directly proportional to BW. As shown in Fig.2, when the value of R8 is 9.50kΩ (95% of R8 maximum), Q value decreases and BW gets wider, which means the notch depth of the center frequency gets deeper (-51.369dB). Whereas when the value of R8 decreases (5% of R8 maximum), Q value increases and BW gets narrower, meaning that the notch depth of the center frequency decreases (-26.021dB). And it is adjustable dependent on the frequency features of the measured biosignal.

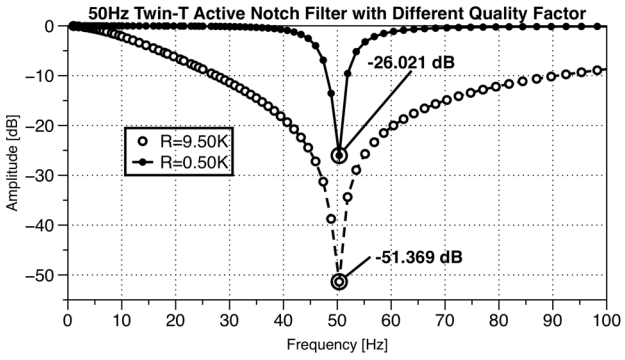

Fig. 2. The notch depth of the 50Hz twin-T active notch filter compared with different quality factors.

D. Fully-Differential Instrumentation Amplifier

A high-precision, low-power, low-noise, rail-to-rail instrumentation amplifier AD8422 (Analog Devices, Inc.) is used and designed in the fully-differential configuration in our active electrode. AD8422 delivers $8\text{nV}/\sqrt{\text{Hz}}$ input voltage noise with 330 μA quiescent current and 2.2MHz bandwidth, making it an ideal choice for measuring a broad spectrum of low level signals [10]. Gain (G) of AD8422 could be set from 1 to 1000 by a single resistor RG. With 80 dB minimum CMRR when G=1 and 150 dB minimum CMRR when G=1000, AD8422 is well suited for extracting low level signals in the presence of high frequency common mode noise. In our design, by switching different values of RG (4 kΩ maximum), variable gains (5.95~1000) could be realized, calculated as $G = 1 + \frac{19.8\text{K}}{\text{RG}}$ [10].

The right-leg driven signal RL recorded by a reference electrode is introduced to the reference terminal of AD8422, which is used to precisely control and maintain the common-mode output voltage at the same level as the reference voltage RL. Then V_{out+} and V_{out-} swing symmetrically around the reference voltage RL. Thus, the differential output voltage $V_{DIFF-OUT}$, defined as the difference between the voltages at the positive and negative output, is set by

$$V_{DIFF-OUT} = V_{out+} - V_{out-} = G \times (V_{in+} - V_{in-}) \quad (5)$$

The common-mode output voltage V_{CM-OUT}, defined as the average of the two output voltages, is set by

$$V_{CM-OUT} = \frac{V_{out+} + V_{out-}}{2} = RL \quad (6)$$

Besides, resistive or capacitive loading could also introduce additional phase lag. To guarantee stability, the value of the capacitor C4 is determined by considering the small signal pulse response of the circuit with load at the extremes of the output dynamic range [11]. And a precision, low noise and bias current operational amplifier ADA4177 (Analog Devices, Inc.) is chosen for cooperation with AD8422 in fully-differential configuration.

Thus the single-ended output signals from the previous notch stage convey to the positive input (V_{ini+}) of the instrumentation amplifier AD8422 and then convert to the differential output signals V_{out+} and V_{out-}. It should be noted that the negative input (V_{ini-}) of AD8422 is connected with 0V standard voltage. The main advantages of the fully-differential configuration are discussed in details as follows:

1) Improve DC precision: DC differential accuracy depends on AD8422, not on the operational amplifier or the resistors. Although the resistor matching of the operational amplifier affect the DC performance like DC common-mode output accuracy, such errors could be possibly rejected by the

next device in the signal chain and thus have little effect on overall system performance [11].

2) Increase noise immunity: As noises coupled into conductors mostly appear as common-mode voltages, thus the fully-differential structure rejects the coupled noises at the differential input, output and the dual power supply (±5V), which increase immunity to external noises [9].

3) Increase output voltage swing: As a result of the change in phase between the differential outputs, the output voltage swing increases by a factor of 2 compared against a single-ended output with the same voltage swing, which is ideally suited for low voltage measurement applications [9].

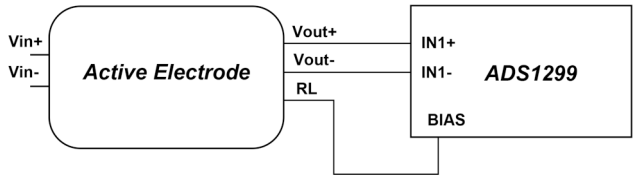

Fig. 3. A diagram of the proposed active electrode in the fully-differential configuration with differential inputs and outputs driving ADS1299.

4) Drive differential ADC inputs: The low noise and distortion, large bandwidth with differential outputs makes AD8422 suited for driving an ADC in a data acquisition system that requires front-end gain, high CMRR and DC precision. Fig. 3 shows AD8422, in the fully-differential configuration, driving ADS1299, an eight-channel, 24-bit, low-noise, low-power ADC with data rates from 250 SPS to 16 kSPS. Besides, each channel of ADS1299 integrates one programmable gain amplifier (PGA), so that the PGA gain could be chosen from one of seven settings (1,2,4,6,8,12 and 24) [12]. Thus, in combination with the previous amplification gain, the overall gain of recording signal would be large enough for high quality measurements. Furthermore, integrating various EEG-specific functions also makes ADS1299 well suited for high performance biosignal especially EEG measurement applications. As shown in Fig. 3, the differential outputs of the fully-differential amplifier, V_{out+} and V_{out-} are connected with IN1+ and IN1-, the positive and negative inputs of channel 1 in ADS1299 respectively. In addition to connecting the positive input of the operational amplifier ADA4177, the right-leg driven signal RL recorded by the reference electrode is also connected with the BIAS terminal of ADS1299 so that the common-mode voltage of human body and the bias output voltage in ADS1299 could remain the same. So as the output common-mode voltage of the fully-differential amplifier matches the voltage RL, the input signal to the ADS1299 could also swing symmetrically about RL to utilize the full dynamic range of the converter [9]. Furthermore, the differential outputs are also ideally suited for the low-pass antialias filter for ADS1299 with differential inputs [9].

III. Experimental Results and Discussions

A. Experimental Setup

The proposed active electrode was built and tested for the performance. The active electrode achieved 4.52 μVrms (0.5 – 200 Hz) input referred noise and 96.09 dB CMRR at 10Hz. Two verification experiments were preliminarily conducted by measuring ECG and EMG signals of 4 subjects with passive electrodes and active electrodes respectively for comparison. The outputs of the electrodes were connected to ADS1299. Then the sampling data was transferred to the Arduino/Teensy microcontroller (PJRC, Inc.) and was finally sent to the computer. Sampling rate was set the same for both the passive electrodes and active electrodes. The experimental protocols were approved by the Ethics Committee for Human Research, Shenzhen Institutes of Advanced Technology, Chinese Academy of Sciences.

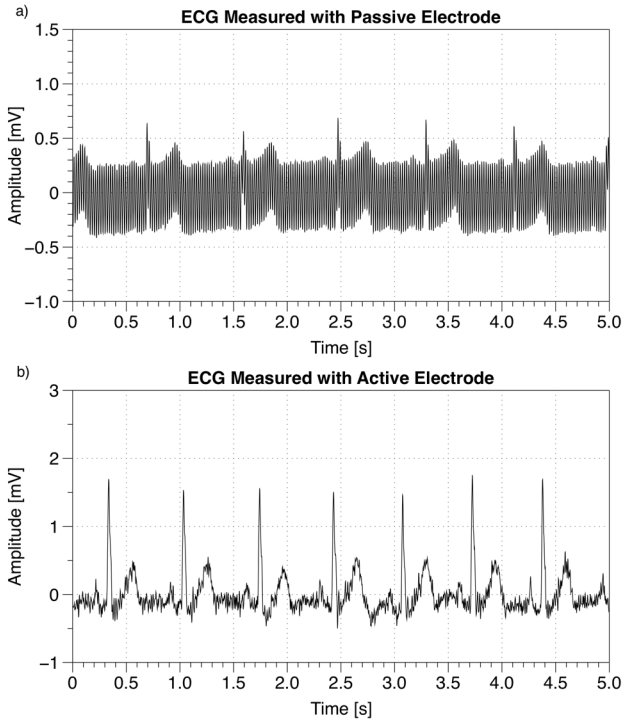

Fig. 4. ECG signals measured from a subject with passive electrode and active electrode are shown in a) and b) respectively.

B. ECG Measurements

In the experiment, the active electrodes including positive input electrode (V_{in+}) and the reference electrode (RL) was placed on the left arm of each subject, while the negative input electrode (V_{in-}) was placed on the right arm. For comparison, three passive electrodes corresponding with V_{in+}, V_{in-} and RL were placed on the same positions as the active electrodes. Fig.

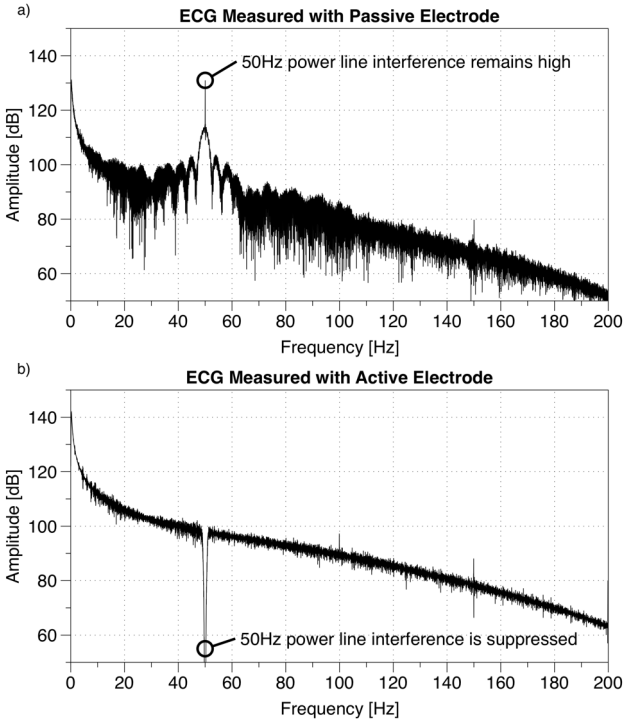

Fig. 5. Spectrums of ECG signals measured with passive electrode and active electrode are shown in a) and b) respectively.

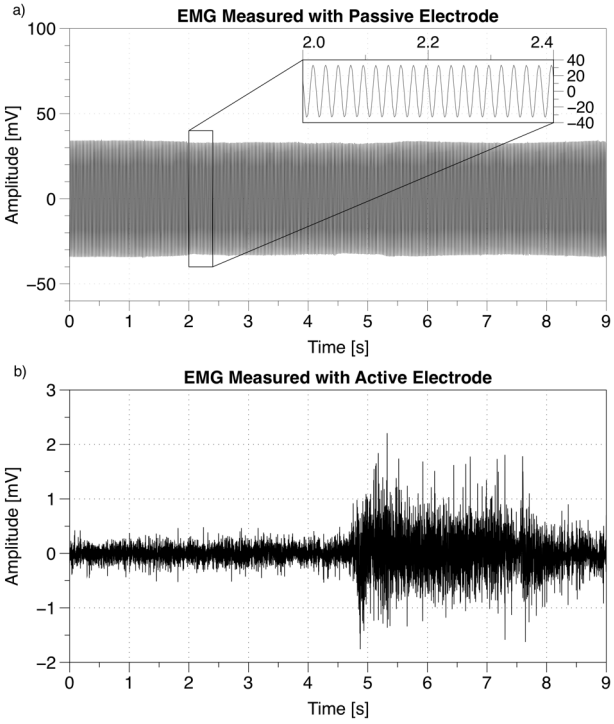

Fig. 6. EMG signals measured from a subject with passive electrode and active electrode are shown in a) and b) respectively. The first 5 seconds are for rest and the next 4 seconds are for clenching the fist.

4 shows the ECG signals of one subject measured with the above two types of electrodes. It's obvious that the ECG signals measured with active electrodes were amplified to approximately 2 mVpp compared with 1 mVpp measured by passive electrodes. Moreover, P, Q-R-S and T waves could be clearly observed in the ECG signals measured with active electrodes. Fig. 5 shows the spectrums of the ECG signals measured by the passive electrodes and the active electrodes accordingly. It could be easily observed from Fig. 5(a) that there is a main peak at 50Hz, thus indicating that the ECG signals measured with passive electrodes suffer heavy power-line interference under no shielding circumstance. While in Fig. 5(b) there is a notch at 50Hz since a 50Hz twin-T active notch filter was integrated in the active electrodes. With the fully-differential configuration of active electrodes as well, the SNR of signals measured is improved and maintained at a high level even without shielding, thus solving the problem without the need of expensive shielded cables.

C. EMG Measurements

In the second experiments, EMG signals were measured when subjects were asked to rest for 5 seconds and clench the fists for 4 seconds. The positive and negative input active electrodes (V_{in+}, V_{in-}) were placed at the brachioradialis of left arm. The reference electrode (RL) was placed at the right ear lobe, which kept as far as possible away from the activated muscle to offer a stable common-mode voltage for reference. Passive electrodes were placed at the same position as the active electrodes. Fig. 6 shows the EMG signal measured with the two types of electrodes. Changes of EMG between the rest and the activation of muscle could be clearly observed from Fig. 6(b),

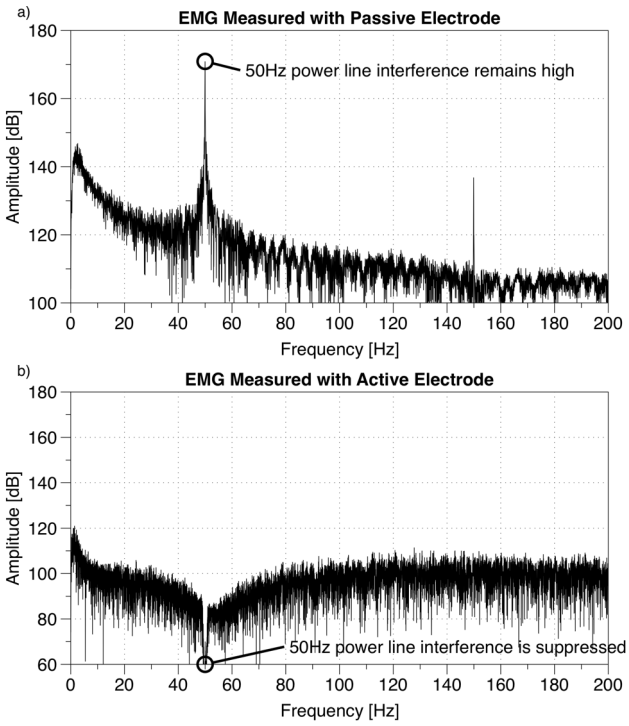

Fig. 7. Spectrums of EMG signals measured with passive electrode and active electrode are shown in a) and b) respectively.

while it's hard to observe from Fig. 6(a) since the SNR of EMG signals measured with passive electrodes without shielding is poor. Fig. 7 shows the spectrums of EMG signals measured with

passive electrodes and active electrodes. In Fig. 7(a), a high peak at 50Hz could also easily be observed with its third harmonics at 150Hz, thus heavily affects the quality of measured EMG by using passive electrodes with no shielding. Contrarily, for EMG measured with active electrodes, 50Hz power-line interference and its harmonics were suppressed thanks to the fully-differential configuration with right-leg driven signal introduced, thus further improving the common-mode noises rejection like power-line interference, as shown in Fig. 7(b). Therefore, the SNR of EMG measured with active electrodes is much higher than passive electrodes without shielding.

Through the above two verification experiments of ECG and EMG measurements using the passive electrodes and the proposed active electrodes, it could be demonstrated that the proposed active electrode contributes to the main interference suppression like power-line interference and motion artifacts, thus improving the SNR of measured signals. However, this paper only includes two preliminary verifications of ECG and EMG. Measurements of ABR, one of the weakest EEG signals have not yet been included in this paper. Thus, using the proposed active electrode to measure and extract the low-level ABR signals (less than 1 μV) or other weak biosignals is the further work we need to finish in the future.

IV. Conclusion

This paper presented a high-performance, low-noise active electrode design for weak biosignal measurements. The proposed active electrode consists of three parts, a difference operational amplifier for impedance match, a 50Hz twin-T active notch filter with adjustable notch depth for power-line interference reduction, and a fully-differential instrumentation amplifier with right-leg driven signal for further common-mode interference rejection. Furthermore, the fully-differential configuration that contains two differential inputs and outputs making the proposed active electrode ideally suited for driving ADS1299 with differential inputs to measure high quality biosignal, which is seldom included in the previous design of active electrodes. The input referred noise of the active electrode was 4.52 μVrms (0.5 – 200 Hz) and the CMRR was 96.09 dB at 10 Hz after testing. Two preliminary verification experiments of ECG and EMG were conducted using the traditional passive electrodes and the proposed active electrodes for comparison. The results demonstrated the benefits of the active electrode in terms of main interference suppression like power-line interference and motion artifacts over the passive electrode. Therefore, the proposed active electrode with low noise and high CMRR could be used for measuring and monitoring 1 μV level biosignal like ABR in the future.

Acknowledgment

This work was supported in part by the National Natural Science Foundation of China under grants (#61302037, #61135004, #61603375, # 51305436), the National Key Basic Research Program of China (#2013CB329505), the Natural Science Foundation of Guangdong Province (#2016A030313179), the Shenzhen Governmental Basic Research Grants (#JCYJ20140610152828679, #JCYJ20140411094009911) and Shenzhen High-level Oversea Talent Program (Peacock Plan) (#KQJSCX20160301141522527).

References

[1] J. Xu, R. F. Yazicioglu, B. Grundlehner, P. Harpe, K. A. A. Makinwa, and C. V. Hoof, "A 160 μW 8-Channel Active Electrode System for EEG Monitoring," IEEE Transactions on Biomedical Circuits and Systems, vol. 5, pp. 555-567, 2011.

[2] A. C. MettingVanRijn, A. P. Kuiper, T. E. Dankers, and C. A. Grimbergen, "Low-cost active electrode improves the resolution in biopotential recordings," in Engineering in Medicine and Biology Society, 1996. Bridging Disciplines for Biomedicine. Proceedings of the 18th Annual International Conference of the IEEE, 1996, pp. 101-102 vol.1.

[3] B. Alizadeh-Taheri, R. L. Smith, and R. T. Knight, "An Active, Microfabricated, Scalp Electrode-array For EEG Recording," in Solid-State Sensors and Actuators, 1995 and Eurosensors IX.. Transducers '95. The 8th International Conference on, 1995, pp. 67-70.

[4] Biosemi [Online]. Available: http://www.biosemi.com/faq/shielding%20vs%20active%20electrodes.htm

[5] D. M. D. Ribeiro, L. S. Fu, L. A. D. Carlos, and J. P. S. Cunha, "A Novel Dry Active Biosignal Electrode Based on an Hybrid Organic-Inorganic Interface Material," IEEE Sensors Journal, vol. 11, pp. 2241-2245, 2011.

[6] C. R. Merritt, H. T. Nagle, and E. Grant, "Fabric-Based Active Electrode Design and Fabrication for Health Monitoring Clothing," IEEE Transactions on Information Technology in Biomedicine, vol. 13, pp. 274-280, 2009.

[7] O. T. Inan and G. T. A. Kovacs, "An 11 μW, two-electrode transimpedance biosignal amplifier with active current feedback stabilization," IEEE Transactions on Biomedical Circuits and Systems, vol. 4, pp. 93-100, 2010.

[8] M. J. Burke and D. T. Gleeson, "A micropower dry-electrode ECG preamplifier," IEEE Transactions on Biomedical Engineering, vol. 47, pp. 155-162, 2000.

[9] Fully-Differntial Amplifiers [Online]. Available: http://www.ti.com/lit/an/sloa054d/sloa054d.pdf

[10] AD8422 [Online]. Available: http://www.analog.com/media/en/technical-documentation/data-sheets/AD8422.pdf

[11] AD8421 [Online]. Available: http://www.analog.com/media/en/technical-documentation/data-sheets/AD8421.pdf.

[12] ADS1299 [Online]. Available: http://www.ti.com/lit/ds/symlink/ads1299.pdf.